iopscience.iop.org

Home Search Collections Journals About Contact us My IOPscience

Nonlinear alfvénic fast particle transport and losses

This article has been downloaded from IOPscience. Please scroll down to see the full text article.

2012 J. Phys.: Conf. Ser. 401 012022

(http://iopscience.iop.org/1742-6596/401/1/012022)

View the table of contents for this issue, or go to the journal homepage for more

Download details:
IP Address: 219.220.216.79
The article was downloaded on 08/02/2013 at 01:29

Please note that terms and conditions apply.

Nonlinear alfvénic fast particle transport and losses

M Schneller[1], Ph Lauber[1], M García-Muñoz[1], M Brüdgam[1] and S Günter[1]
[1] Max Planck Institute for Plasma Physics, EURATOM Association, Boltzmannstr. 2, 85748 Garching, Germany

E-mail: `mirjam.schneller@ipp.mpg.de`

Abstract. Magnetohydrodynamic instabilities like Toroidal Alfvén Eigenmodes or core-localized modes such as Beta Induced Alfvén Eigenmodes and Reversed Shear Alfvén Eigenmodes driven by fast particles can lead to significant redistribution and losses in fusion devices. This is observed in many ASDEX Upgrade discharges. The present work aims to understand the underlying resonance mechanisms, especially in the presence of multiple modes with different frequencies. Resonant mode coupling mechanisms are investigated using the drift kinetic HAGIS code [Pinches 1998].
Simulations were performed for different plasma equilibria, in particular for different q profiles, employing the availability of improved experimental data. A study was carried out, investigating double-resonant mode coupling with respect to various overlapping scenarios. It was found that, depending on the radial mode distance, double-resonance is able to enhance growth rates as well as mode amplitudes significantly. Small radial mode distances, however can also lead to strong nonlinear mode stabilization of a linear dominant mode.
With the extended version of HAGIS, losses were simulated and directly compared with experimental loss measurements. The losses' phase space distribution as well as their ejection signal is consistent with experimental data. Furthermore, it allowed to characterize them as prompt, resonant or stochastic. It was found that especially in multiple mode scenarios (with different mode frequencies), abundant incoherent losses occur in the lower energy range, due to a broad phase-space stochastization. The incoherent higher energetic losses are "prompt", i.e. their initial energy is too large for confined orbits.

1. Introduction

Fusion devices contain fast particle populations due to external plasma heating and (eventually) fusion-borne α-particles. Fast particle populations can interact with global electromagnetic waves, leading to the growth of MHD-like and kinetic instabilities – e.g., Toroidicity Induced Eigenmodes (TAE) [1], Reversed Shear Alfvén Eigenmodes (RSAE) [2] or Beta Induced Alfvén Eigenmodes (BAE) [3]. In this work, drift-kinetic fast particle simulations performed with the HAGIS code [4] are carried out to obtain a deeper understanding of the dynamics of wave-fast particle interaction in scenarios with two modes of different frequencies: what is the mode coupling mechanism, and how does it dependent on radial mode distance? In a second study, the extended version of HAGIS [5] is used to simulate fast particle losses and to compare them with experimental loss measurements [6] in ASDEX Upgrade (AUG). The losses' phase space distribution as well as their ejection signal allows to characterize them as prompt, resonant or stochastic.

2. Simulation Tool and Experimental Reference Case

The numerical investigations are performed with the HAGIS Code [4], a nonlinear, drift-kinetic, perturbative Particle-in-Cell code, that models the interaction between a distribution of energetic

Published under licence by IOP Publishing Ltd

particles and a set of Alfvén Eigenmodes. The plasma equilibrium for HAGIS is based on the CLISTE [7] and HELENA [8] codes. The data for the MHD equilibria originate from the ICRH minority heated ASDEX Upgrade discharge #23824, at times $t = 1.16$ s and $t = 1.51$ s. At the earlier time point, the q profile is slightly inverted ($q_0 = -1.55$, $q_{\mathrm{min}} = -1.43$) at the later time point, it is monotonic, with lower absolute values ($q_0 = q_{\mathrm{min}} = -0.97$)[1]. This particular reference scenarios were chosen due to the availability of detailed experimental data concerning fast particle-wave interaction and losses. The comparison between these data and numerical results is subject of section 4.

3. Numerical Study on Double-Resonance

Theoretical Picture Theory (e.g. Ref. [9]) predicts that conversion of free energy to wave energy is enhanced in a multiple-mode scenario, i.e., the interaction of multiple modes produces energy conversion rates higher than that which would be achieved with each mode acting independently. This effect is called “double-resonance” and can be partially explained by the principle of gradient driven mode growth – according to[2]: $\gamma \propto \nabla f(s)$ [10] – which can be extended to multiple modes [9, 11]. This picture of ***gradient driven double-resonance*** is based on the precondition that modes share resonances in the same phase space area. Through the resulting redistribution by each mode, a steeper gradient is produced at the other mode’s position, enhancing its drive. The radial overlapping of modes leads then to a much larger conversion of free energy to wave energy.

However, this mechanism can only work if the modes not only share resonance regions in phase space, but if there is also *spatial* mode overlap in the radial direction. In Ref. [5] simulations were carried out, finding a double-resonant effect also without this precondition. Furthermore, a superimposed oscillation on the modes’ amplitudes was observed, clearly indicating mode-mode interaction. The modes without radial overlap are then coupled radially through the particles’ trajectories: A population of particles that shares resonances in phase space with both modes and passes both modes’ location at once, can transfer energy from one mode to the other [5]. Due to the particle orbits’ width, it is not necessary that both modes have a radial overlap. In the following, this mechanism is called ***inter-mode energy transfer***.

Simulation Conditions As the first question, the understanding of double mode resonance is very fundamental, the simulations were performed under quite simple physical conditions: radial particle distribution $f(\psi)$ with constant gradient (to avoid different mode drive at different radial mode positions only due to a steeper gradient) and a slowing down function as energy distribution function. The volume averaged fast particle beta is β_{f}=1%. The particles are distributed isotropically in pitch angle (as e.g., fusion borne α-particles would be).

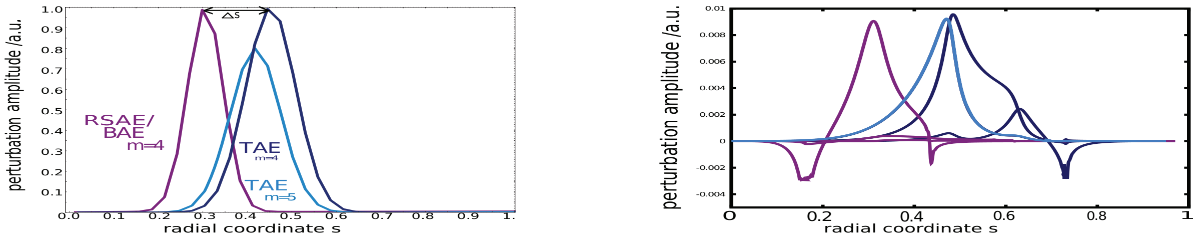

(a) analytical perturbation (b) numerical perturbation

Figure 1: *Two Alfvénic modes: (a) gauss-shaped perturbation as used in the following simulations, (b) for comparison: perturbations occurring in AUG discharge #23824, as calculated numerically with* LIGKA *[12].*

---

[1] Note that the q profile is negative here, due to the AUG current direction.

[2] s refers to the radial coordinate as the square root of the normalized poloidal flux: $s = (\psi_{\mathrm{pol}}/\psi_{\mathrm{pol,edge}})^{1/2}$.

As MHD perturbations, analytic, gauss shaped functions are used (see figure 1), without background damping. The mode frequencies are chosen to match experimental data: one high frequency mode 120 kHz (TAE) and one lower frequency mode at 55 kHz (possible RSAE or BAE).

Simulation Results A scan over the radial mode distance reveals an effective double-resonance as shown in figure 2: depicted are the ratios of the linear growth rates (a) and the amplitudes (b) in the double mode case vs. the single mode case over the radial mode distance Δs. The amplitude level was compared after ≈ 300 TAE periods ($= 2.5$ ms) of simulation time. This time is sufficient for the single amplitudes to saturate, but still significantly below energy slowing down time. One can see that the **growth rates** of both the TAE and the RSAE are enhanced in all double mode cases compared to the single mode ones. However, the growth rate of the outer TAE is enhanced most strongly and independently of the radial mode distance – i.e. gradient driven double-resonance works even if there is no radial mode overlap. In contrast, the enhancement of the inner and weaker RSAE decreases with the radial mode distance for small Δs. Then it increases again for $\Delta s > 0.15$. These larger mode distances match the double-resonant particle orbits and therefore enable intermode energy exchange, driving the weak mode. For higher Δs, the larger, i.e. higher energetic orbits fit the mode distance and lead to even more energy exchange. Furthermore, with larger radial mode distances, the modes are able to tap energy from a wider gradient region. The **amplitude** ratios, however, are even lowered in the double-resonant case compared to the respective single mode levels, if the radial mode distance is small. This happens due to the mutual gradient depletion at the other mode's radial position. If the modes are at a larger radial distance ($\Delta s > 0.15$), the double mode scenario amplitudes are much higher compared to the single mode amplitudes, both for the TAE and the RSAE. Both modes drive each other – most for a radial distance of about $\Delta s \approx 0.25$.

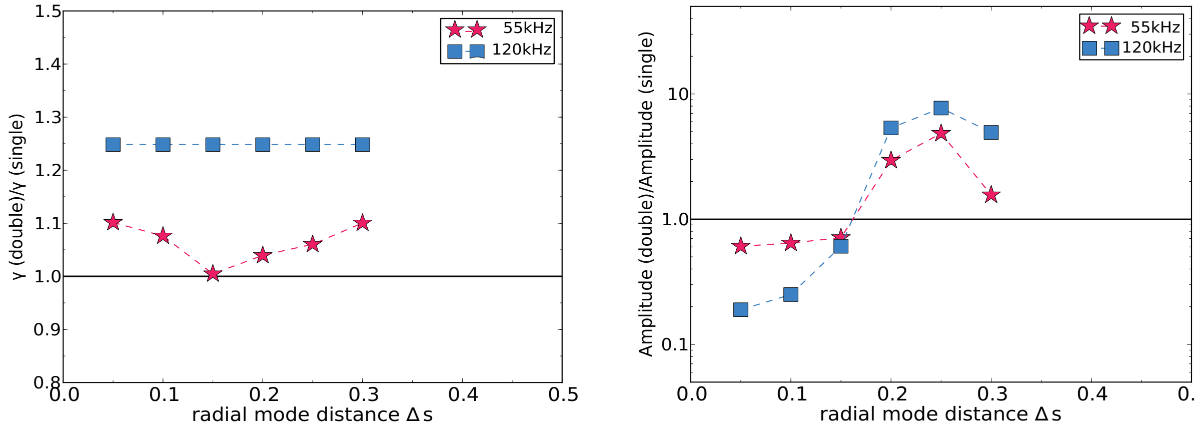

(a) *Growth rates enhancement* (b) *Amplitudes enhancement (at $t \approx 300$ T)*

Figure 2: *Mode evolution scanned over the radial mode distance Δs in the inverted q profile case. Depicted is the Δs dependence of the ratios of growth rates (a) and amplitudes (b) in double mode simulations over those from single mode simulations. Red star: RSAE, blue square: TAE. One can clearly see that larger radial mode distances lead to higher amplitudes, whereas amplitudes are even lower than in the single mode case for $\Delta s \leq 0.15$. The linear growth rates, however, are higher than in the single mode simulation throughout the Δs range. The RSAE growth rate experiences a small drop at $\Delta s \approx 0.15$.*

It is important to note that the distance $\Delta s = 0.25$ giving maximum amplitude ratios depends strongly on the absolute mode positions with respect to the radial distribution function, and especially on the amplitude regime (stochastic or non-stochastic) of each mode. The same applies for the value $\Delta s = 0.15$ at which the transition towards double-resonant amplitude enhancement takes place.

Summary (I) Growth rates are generally enhanced by the presence of another mode, whereas for the amplitudes, this is only the case, if the modes have sufficiently large radial distance. For small distances, modes at radial positions, where the initial distribution function is already relatively flat, double-resonance leads to strong mode stabilization with respect to the single mode case. If the amplitudes are enhanced, their amplification level is, however, mainly determined by whether the mode reaches the stochastic regime. The stochastic threshold is reached much earlier or even only if a second mode is present.

4. Fast Particle Losses in Numerical Simulations vs. Experimental Measurements

Experimental Loss Observations In the AUG discharge #23824, during the inverted q profile equilibrium at $t = 1.16$ s, a high loss signal is observed at the Fast Ion Loss Detector (FILD), with the majority of losses characterized as *incoherent*. Later, at $t = 1.51$ s, during the monotonic q profile equilibrium, only very few losses occur, and all are identified as *coherent* [6]. In the following, simulations within this experimental reference frame are presented, that were performed to identify the origin of the different loss types.

Simulation Conditions The simulations presented in this section are carried out with an extended HAGIS version [5], including the vacuum region, and are based on more realistic plasma conditions: The radial particle loading follows a Fermi-like potential law $f(s) = (1 - s^2)^5$, that decays to zero at $s = 0.6$. It was chosen in a way that does not produce prompt losses in the simulations with monotonic q profile, as seen in the experiment. Furthermore, the markers are initialized in pitch and poloidal angle distribution according to an analytical function that models the distribution created by ICRH (main heating method in AUG #23824). β_f is set to 0.1%. As MHD perturbation, the analytic, gauss functions (figure 1) are used, without background damping. The mode frequencies, positions and widths are chosen to be consistent with experimental data: at $t = 1.16$ s, a 120 kHz TAE at $s = 0.45$ and a 55 kHz RSAE at $s = 0.35$, whereas at $t = 1.51$ s, there is a TAE of 180 kHz at $s = 0.6$ and a BAE of 80 kHz at $s = 0.35$ [13]. These data were obtained from Fourier spectrograms of the SXR signal, Mirnov Coils and the FILD signal [14].

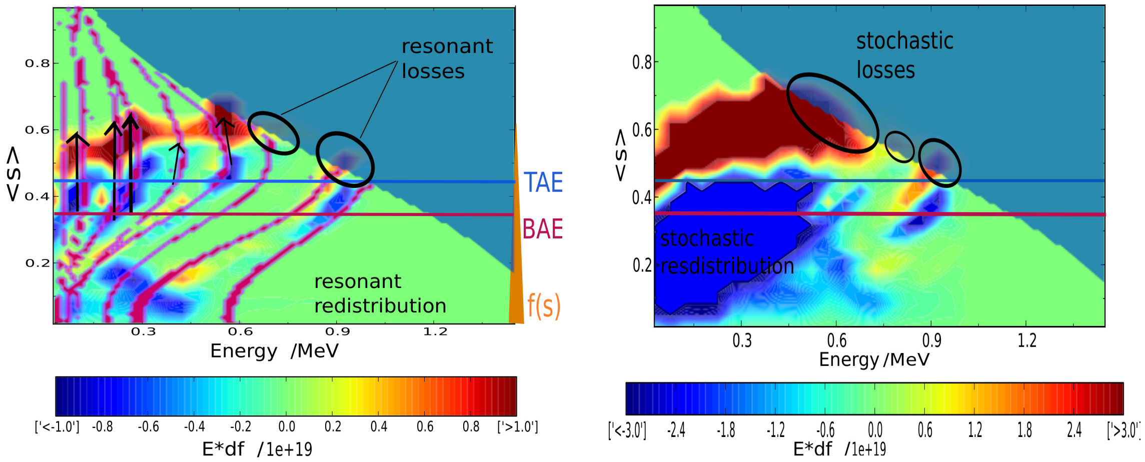

(a) *redistribution in phase space*

(b) *losses in phase space*

Figure 3: *Double mode simulation in the inverted q profile equilibrium: Redistribution in E-s space during (a): redistribution phase (t ≈ 0.6 ms), (b) stochastic phase (t ≈ 1.8 ms) Red: particles accumulate, blue: particles move away. One can see the good accordance of redistribution areas (black arrows) and the resonance lines (pink) in the modes' vicinity (horizontal lines). The redistribution in the areas, where the resonance lines meet the loss boundary (black circles) coincide with the losses (see figure 4a).*

Simulation Results Consistent with results from the numerical study, it is found that the mode amplitudes grow slower with the monotonic q profile and do not reach the stochastic threshold (at $\approx 2 \cdot 10^{-3} \delta B/B$). A superimposed oscillation frequency is visible in both scenarios, originating from the double-resonance mechanism of inter-mode energy exchange. Its frequency matches with the beat frequency of both modes. In the inverted q profile, the modes reach the stochastic regime. There, particle redistribution in phase space takes place broadly over the whole energy range (figure 3b) at the modes' radial position. Slightly before, during the resonant phase, however, redistribution in phase space occurs along the resonance lines (figure 3a). The energy of the losses obtained during this "redistribution phase" (see figure 4a) matches roughly with the energy, at which the higher resonance lines meet the loss boundary. This indicates, that losses in this time period are *resonant*, i.e. *coherent* losses. In the simulation with the monotonic q profile, there is no redistribution into the loss region. Thus, very few losses appear, consistent with experimental measurements.

To learn more about the identity of the *incoherent* losses, their **phase space pattern** is analyzed in the following. The distribution function of the fast particles is not known exactly, therefore, the markers are loaded according to an estimated distribution function. To learn how sensitive the loss pattern is with respect to the parameters defining the distribution function, a scan is performed over the radial, as well as over the poloidal distribution function. Combining the results of both the radial and the poloidal marker loading scan, it turns out that there is a phase space region that cannot be covered by prompt losses in neither loading scenario: the phase space region of energies below 600 keV (45 mm gyroradius) at negative pitch angles smaller than 63°. These losses are very likely to be stochastic losses. For the rest of the phase space, it is not possible to discern prompt from later losses yet.

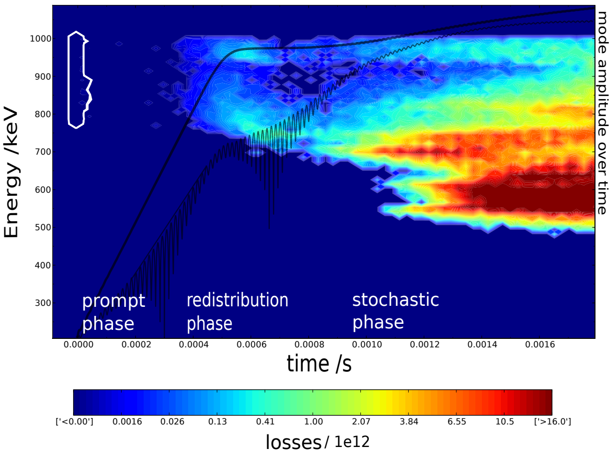

Figure 4: *Lost particles at the first wall over simulation time in the inverted q profile: in the stochastic phase, losses spread over a large energy range, even to lower energies around 500 keV. For comparison, the edge of the phase space region of the prompt losses in this simulation is shown (white lines). Black lines: amplitude evolution of RSAE (upper) and TAE (lower).*

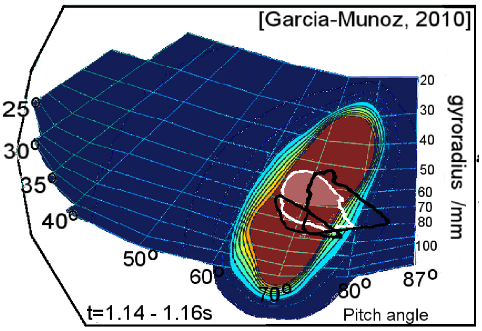

Figure 5: *Fast ion losses in phase space (AUG discharge #23824): colors give the FILD measured loss pattern [6], lines give the boundary of the numerical calculated loss region. Black lines: upper estimate for the (drift corrected) border of the prompt losses appearance resulting from the radial and poloidal marker loading scan. White lines: same for the losses during the stochastic phase of the MHD perturbations. The lighter shaded area indicates the peak region of stochastic losses.*

Figure 5 shows the good accordance of the numerically calculated losses and the experimentally measured ones: the whole loss area as well as the peak region of the numerical values lies almost entirely within the respective experimentally measured region of phase space. The experimental peak being slightly broader results mainly from over exposure of the FILD loss plate. The higher energetic losses (i.e. the pattern at gyroradii > 90 mm or energy > 1 MeV) do not appear in the simulation, as the fast particle energy was cut at 1 MeV. The lower energetic losses below 50 mm

gyroradius are expected to appear when simulating with more than two modes at lower frequencies (work in progress).
When looking closely at the loss time traces, one can perceive an ejection modulation. A **Fourier analysis of the loss signal** gives a peak at 65 kHz, which is exactly the beat frequency. In the above simulation, the mode frequencies result in beat frequencies of 65 kHz and 175 kHz. Unfortunately, the RSAE frequency is very close to the lower beat frequency, and the TAE frequency almost coincides with the first harmonic of it. Therefore, another simulation was performed, using $\omega_{\mathrm{RSAE}} = 70$ and $\omega_{\mathrm{TAE}} = 100$ kHz. A Fourier analysis of the loss signal is performed for the resonant phase (figure 6a), and the stochastic phase (figure 6b). In the resonant phase, the RSAE frequency peak at around 70 keV is visible, whereas the TAE's amplitude is still too small to produce significant losses. Later on in the simulation, the TAE grows towards the same amplitude range as the RSAE, likewise, the beat frequency peak becomes visible in the Fourier spectrum. This is consistent with FILD spectra, showing the beat frequency as well.

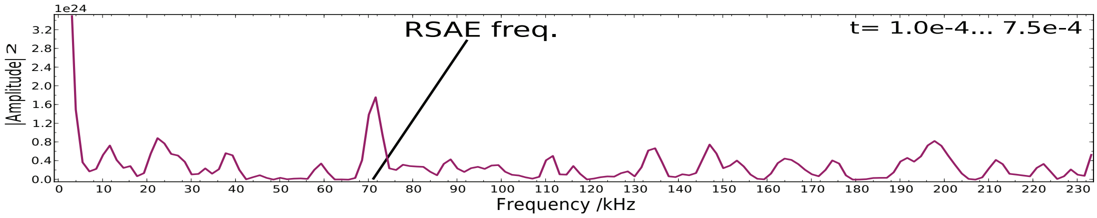

(a) *FFT of losses' time signal during resonant phase*

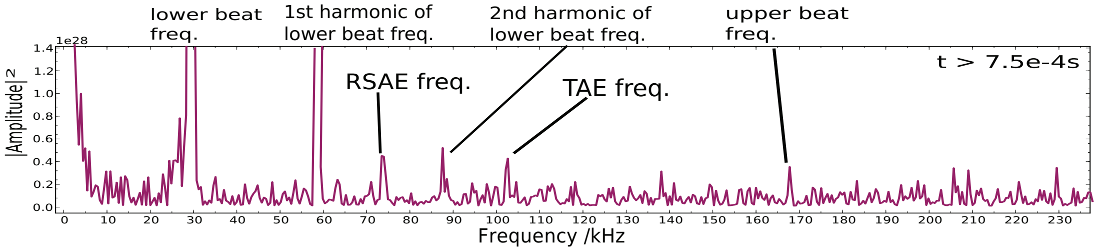

(b) *FFT of losses' time signal during stochastic phase*

Figure 6: *Fourier spectra of losses time signal. (a) in the resonant phase: a significant number of particles is ejected with the frequency of the dominating RSAE (70 kHz). (b) in the stochastic phase: the beat frequency (30 kHz) is by far dominating (and its higher harmonics). All frequencies experience a slight down-shift.*

Summary (II) With the extended version of Hagis, losses were simulated and compared with experimentally observed losses at the Fast Ion Loss Detector. The simulated losses' phase space pattern coincides very well with the experimental one. Especially in multi-mode scenarios with different mode frequencies, stochastic redistribution sets in over a broad energy range, leading to lower energetic losses, that are incoherent. The resonant losses appear from the late linear phase on, mainly in the high energy regime, showing good coherence with the modes' frequencies and especially their beat frequencies. The higher energetic part of experimentally measured incoherent losses was identified as mainly prompt losses. The internal redistribution, as well as the losses can be understood very well as processes in phase space, when combining resonance lines, loss boundary and radial positions of the Alfvénic modes.

References

[1] Cheng C Z, Chen L and Chance M 1985 *Ann. Phys.* **161** 21 – 47

[2] Berk H L, Borba D N, Breizman B N, Pinches S D and Sharapov S E 2001 *Phys. Rev. Lett.* **87**

[3] Heidbrink W W, Strait E J, Chu M S and Turnbull A D 1993 *Phys. Rev. Lett.* **71**(6) 855–858

[4] Pinches S, Appel L, Candy J, Sharapov S, Berk H, Borba D, Breizman B, Hender T, Hopcraft K, Huysmans G and Kerner W 1998 *Comput. Phys. Commun.* **111** 133 – 149

[5] Brüdgam M 2010 Ph.D. thesis Technische Universität München

[6] García-Muñoz M et al 2010 *Phys. Rev. Lett.* **104**(18)

[7] Mc Carthy P J and the ASDEX Upgrade Team 2012 *Plasma Phys. Control. Fusion* **54** 015010

[8] Huysmans G T A et al 1990 Conf. on Computational Physics Proc. World Scientific, Singapore (AIP)

[9] Berk H L, Breizman B and Ye H 1992 *Phys. Rev. Lett.* **68**(24) 3563–3566

[10] Fu G Y and Dam J W V 1989 *Phys. Fluids B* **1** 1949–1952

[11] Berk H L and Breizman B N 1990 *Phys. Fluids B* **2** 2226–2252

[12] Lauber Ph, Günter S, Könies A and Pinches S D 2007 *J. Comp. Phys.* **226** 447 – 465

[13] Lauber Ph et al 2009 *Plasma Phys. Control. Fusion* **51** 124009

[14] García-Muñoz M et al 2011 *Nuclear Fusion* **51**